

QCD effective charges and the proton structure function at small- x [†]

Emerson Luna

Universidade Federal do Rio Grande do Sul

VII ONTQC

Oficina Nacional de Teoria Quântica de Campos

Salvador - BA, 2021

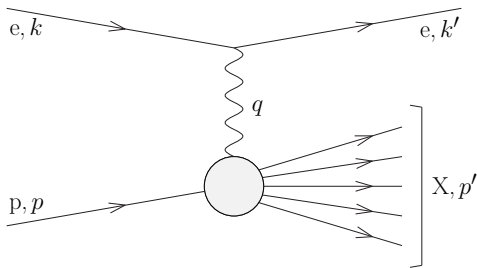
[†] *in collaboration with M. Peláez*

Outline

- $F_2(x, Q^2)$ at low Q^2 and small- x : The necessity of non-perturbative corrections
- Problem of how to incorporate nonperturbative corrections to F_2
- A solution via QCD effective charges
- Higher twist contributions to F_2
- Some results
- Conclusion and Perspectives

■ ep scattering: At large Q^2 inelastic scattering is much more probable

■ The deep-inelastic scattering (DIS) of leptons off nucleons is the instrumental tool for high precision measurements of the quark and gluon content of the nucleons



Inelastic electron-proton scattering

Two basic kinematical variables in the **deep inelastic scattering (DIS)**
electron (k) + proton (p) \rightarrow electron(k') + X (p_X):

$$Q^2 = -q^2 > 0 \quad (\text{virtuality of photon})$$

$$x = \frac{Q^2}{2p \cdot q} = \frac{Q^2}{Q^2 + W^2 - M^2} \quad (\text{Bjorken variable})$$

where $W^2 \equiv (p + q)^2 \geq M^2 \implies 0 \leq x \leq 1$

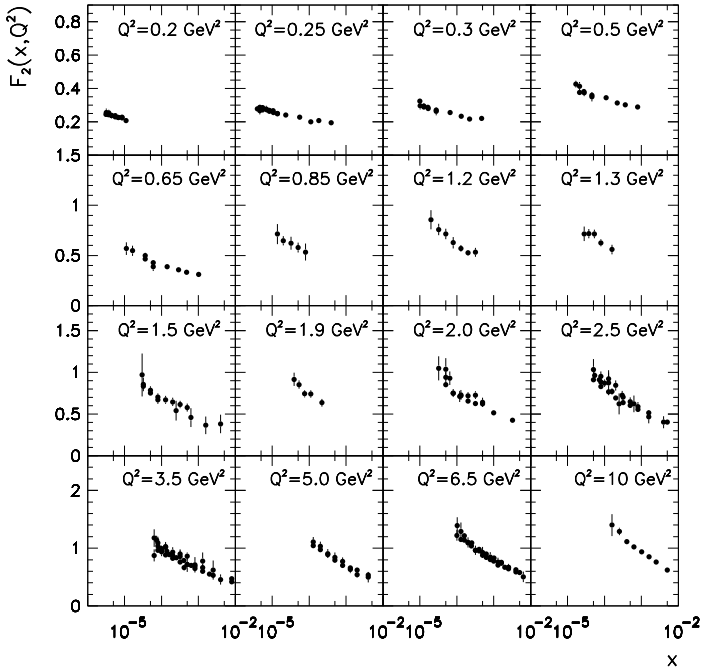
■ High energy limit: $W^2 \gg Q^2 > M^2 \implies x \simeq Q^2/W^2 \ll 1$

■ The nucleon structure function $F_2(x, Q^2)$ at low Q^2 has been measured in the previously unexplored small- x regime at the HERA collider

⇒ a long-standing question is the extent to which the non-perturbative properties of QCD affect the behavior of F_2

⇒ the low Q^2 and small- x regions bring us into a kinematical region where non-perturbative QCD effects becomes essential

These regions are very interesting kinematical domains for testing new QCD theoretical ideas



■ The necessity of non-perturbative corrections arises as follows:

⇒ at sufficiently small x the power series in $\alpha_s \ln(1/x)$ may be resummed via BFKL equation

Resummations in QCD

- Every physical observable can be written, in pQCD, as a power series in α_s
 - ⇒ in these series the coupling constant is accompanied by large logarithms, which need to be resummed
 - ⇒ according to the type and to the powers of logarithms that are effectively resummed one gets different evolution equations
- The solution of the **DGLAP equation** sums over all orders in α_s the contributions from leading, single, collinear logarithms of the form $\alpha_s \ln(Q^2/Q_0^2)$
 - ⇒ it does not include leading, single, soft singularities of the form $\alpha_s \ln(1/x)$, which are treated instead by the **BFKL equation**
- The BFKL equation describes the x -evolution of PDFs at fixed Q^2

Resummations in QCD

■ The phase space regions which contribute these logarithms enhancements are associated with configurations in which successive partons have strongly ordered transverse, k_T , or longitudinal, $k_L \equiv x$, momenta:

$$\Rightarrow \alpha_s L_Q \sim 1, \alpha_s L_x \ll 1: Q^2 \gg k_{T,n}^2 \gg \dots \gg k_{T,1}^2 \gg Q_0^2$$

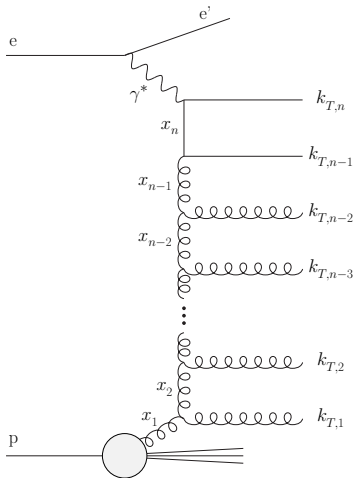
$$\Rightarrow \alpha_s L_x \sim 1, \alpha_s L_Q \ll 1: x \ll x_n \ll \dots \ll x_1 \ll x_0$$

■ At small- x and slow Q^2 (where gluons are dominant) we do not have strongly ordered k_T

\Rightarrow we have to integrate over the full range of k_T

\Rightarrow this leads us to work with the *unintegrated* gluon PDF $\tilde{g}(x, k_T^2)$:

$$xg(x, Q^2) = \int^{Q^2} \frac{dk_T^2}{k_T^2} \tilde{g}(x, k_T^2)$$



Ladder diagrams

■ The result of resumming these leading terms is sensitive to the infrared k_T region and it is found that

$$\tilde{g}(x, k_T^2) \sim C(k_T^2) x^{-\lambda}$$

where $\lambda \sim 0.5$ and $\tilde{g}(x, k_T^2)$ is the *unintegrated* gluon distribution

⇒ the relation between $\tilde{g}(x, k_T^2)$ and $g(x, Q^2)$, the *standard* gluon distribution (to be determined by the analysis of the $F_2(x, Q^2)$ data) reads

$$\tilde{g}(x, k_T^2) = \left. \frac{\partial(xg(x, Q^2))}{\partial \ln Q^2} \right|_{Q^2=k_T^2}$$

■ At this point it is clear that non-perturbative contributions are needed:

⇒ first, the resummation program requires knowledge of the gluon for all k_T^2 including the deep infrared region

⇒ second, the data in the small- x region show that F_2 tend to a flat shape with decreasing Q^2 , particularly for low Q^2

⇒ this indicates that the singular behavior $x^{-\lambda}$ predicted by BFKL must be suppressed by non-perturbative effects

■ Hence approaching the low Q^2 region from the QCD theory makes evident the problem of how to incorporate in an effective way non-perturbative corrections into the description of the structure function F_2

Question: How to address this question?

Leading-twist expansion of F_2

■ Our task of calculating infrared contributions to the QCD description of data on F_2 can succeed in a consistent way by analyzing **exclusively** the small- x region

⇒ in this limit some of the existing analytical solutions of the DGLAP equation can be directly used

⇒ in this approach the **HERA** data at small- x is interpreted in terms of the **double-asymptotic-scaling (DAS)** phenomenon

⇒ The analytical solutions can be extended in order to include the subasymptotic part of the Q^2 evolution

⇒ generalized DAS approximation

⇒ parton distributions evolved from flat x distributions at some starting point Q_0 for the DGLAP evolution

■ The **twist-two** term of $F_2(x, Q^2)$ at NLO is given by [1,2]

$$\frac{1}{e} F_2^{\tau^2}(x, Q^2) = f_q^{\tau^2}(x, Q^2) + \frac{4T_R n_f}{3} \frac{\alpha_s(Q^2)}{4\pi} f_g^{\tau^2}(x, Q^2)$$

⇒ it may be worth emphasizing that this expression is valid only for $x \ll 1$

⇒ the distributions $f_a^{\tau^2}$ are written using a representation which follows from the solution of the DGLAP equation in the Mellin moment space (see [2])

[1] A.Y.Illarionov, A.V.Kotikov, G.Parente, Phys.Part.Nucl.**39**(2008)307;

[2] EGSL, A.L.dos Santos, A.A.Natale, Phys. Lett. B **698** (2011) 52.

Higher-twist corrections

■ In pQCD we make approximations that use the leading power of an expansion in small variables like masses relative to a hard scale Q

⇒ It is natural to ask about the role of non-leading powers

⇒ higher twist corrections to DIS processes have been studied systematically in the framework of the OPE

■ In this scenario the structure functions have *higher-twist* power corrections:

$$F(x, Q^2) = F^{\tau=2}(x, Q^2) + \frac{F^{\tau=4}(x, Q^2)}{Q^2} + \frac{F^{\tau=6}(x, Q^2)}{Q^4} + \dots$$

Some technical difficulties

- There are theoretical difficulties of controlling power corrections in effective theories...

⇒ ... the calculation of power corrections requires the evaluation of the matrix elements of higher-twist operators...

⇒ ... but in order to cancel certain ambiguities it is also necessary to compute the Wilson coefficient functions to sufficiently high orders of the perturbation series

⇒ these '*renormalon*' ambiguities are of the same order as the power corrections

- Fortunately, the twist-4 ambiguity cancels the corresponding ambiguity in the definition of the twist-2 contribution.

■ Unfortunately, it is not clear if the ambiguity of higher twist contributions can also be canceled

⇒ in general only a few terms of the perturbative series are known

⇒ these series are plagued by similar renormalon ambiguities

■ However, the subtle relation between the twist-two and the twist-four contributions has inspired the hypothesis that the main contributions to the matrix elements of the twist-four operators are proportional to their divergent parts

⇒ this means that in practice we can obtain information about power corrections from the large-order behavior of the corresponding series

⇒ this approach is called *infrared renormalon model*.

■ The twist-four (τ^4) correction to $F_2(x, Q^2)$ in the $[R]$ renormalon formalism is given by [3]

$$\begin{aligned} F_2^{[R]\tau^4}(x, Q^2) &= e \sum_{a=q,g} A_a^{\tau^4} \tilde{\mu}_a^{\tau^4}(x, Q^2) \otimes f_a^{\tau^2}(x, Q^2) \\ &= \sum_{a=q,g} F_{2,a}^{[R]\tau^4}(x, Q^2) \end{aligned}$$

\Rightarrow the functions $\tilde{\mu}_a^{\tau^4}(x, Q^2)$ are obtained by means of the infrared renormalon model, and

$$F_2^{[R]}(x, Q^2) = F_2^{\tau^2}(x, Q^2) + \frac{1}{Q^2} F_2^{[R]\tau^4}(x, Q^2)$$

[3] D.Hadjimichef, EGSL, M.Peláez, Phys. Lett. B **804** (2020) 135350.

■ Similarly the twist-six ($\tau 6$) correction to $F_2(x, Q^2)$ reads [3]

$$\begin{aligned} F_2^{[R]\tau 6}(x, Q^2) &= e \sum_{a=q,g} A_a^{\tau 6} \tilde{\mu}_a^{\tau 6}(x, Q^2) \otimes f_a^{\tau 2}(x, Q^2) \\ &= \sum_{a=q,g} F_{2,a}^{[R]\tau 6}(x, Q^2) \end{aligned}$$

⇒ the functions $\tilde{\mu}_a^{\tau 6}(x, Q^2)$ are also obtained by means of the infrared renormalon model

⇒ now, taking into account all higher twist corrections, we have

$$F_2^{[R]}(x, Q^2) = F_2^{\tau 2}(x, Q^2) + \frac{1}{Q^2} F_2^{[R]\tau 4}(x, Q^2) + \frac{1}{Q^4} F_2^{[R]\tau 6}(x, Q^2)$$

■ If $F_2^{[R]h\tau}(x, Q^2)$ denotes the higher-twist operators, we have

$$F_2^{[R]}(x, Q^2) = F_2^{\tau^2}(x, Q^2) + F_2^{[R]h\tau}(x, Q^2),$$

where the “+” and the “-” representations of $F_2^{[R]h\tau}(x, Q^2)$ can each be put into a compact form [3]:

$$\begin{aligned} \frac{1}{e} F_2^{[R]h\tau,+}(x, Q^2) &= \frac{32T_R n_f}{15\beta_0^2} f_g^{\tau^2,+}(x, Q^2) \sum_{m=4,6} k_m \left\{ \frac{A_q^{\tau m}}{Q^{(m-2)}} \left(\frac{2}{\rho} \frac{\tilde{l}_1(\rho)}{\tilde{l}_0(\rho)} + \ln \left(\frac{Q^2}{|A_q^{\tau m}|_{l_m}} \right) \right) \right. \\ &+ \frac{4C_F T_R n_f}{3C_A} \frac{A_q^{\tau m}}{Q^{(m-2)}} \left[\left(1 - \bar{d}_{+-}^q (1) \frac{\alpha_s(Q^2)}{4\pi} \right) \left(\frac{2}{\rho} \frac{\tilde{l}_1(\rho)}{\tilde{l}_0(\rho)} + \ln \left(\frac{Q^2}{|A_q^{\tau m}|_{l_m}} \right) \right) \right. \\ &+ \left. \left. \frac{20C_A}{3} \frac{\alpha_s(Q^2)}{4\pi} \left(\frac{2}{\rho^2} \frac{\tilde{l}_2(\rho)}{\tilde{l}_0(\rho)} + \ln \left(\frac{Q^2}{|A_q^{\tau m}|_{l_m}} \right) \frac{1}{\rho} \frac{\tilde{l}_1(\rho)}{\tilde{l}_0(\rho)} \right) \right] \right\}, \end{aligned}$$

$$\begin{aligned} \frac{1}{e} F_2^{[R]h\tau,-}(x, Q^2) &= \frac{32T_R n_f}{15\beta_0^2} f_g^{\tau^2,-}(x, Q^2) \sum_{m=4,6} k_m \left\{ \frac{A_q^{\tau m}}{Q^{(m-2)}} \ln \left(\frac{Q^2}{x_q^2 |A_q^{\tau m}|_{l_m}} \right) \right. \\ &- \left. 2C_A \frac{A_q^{\tau m}}{Q^{(m-2)}} \left[\ln \left(\frac{1}{x_q} \right) \ln \left(\frac{Q^2}{x_q |A_q^{\tau m}|_{l_m}} \right) - \rho'(\nu_q) \right] \right\}, \end{aligned}$$

with $k_4 = 1$, $k_6 = -8/7$, $l_4 = 1$, and $l_6 = 1/2$.

QCD effective charges

■ The non-perturbative dynamics of QCD may generate an effective momentum-dependent mass $m(q^2)$ for the gluons

⇒ numerical simulations indicate that such a dynamical mass does arise when the non-perturbative regime of QCD is probed

⇒ large-volume lattice QCD simulations, both for $SU(2)$ and $SU(3)$, reveal that the gluon propagator is finite in the deep infrared region

⇒ in the continuum, it turns out that the non-perturbative dynamics of the gluon propagator is governed by the corresponding Schwinger-Dyson equations (SDEs)

⇒ according to the SDEs a finite gluon propagator corresponds to a massive gluon

■ The QCD effective charge $\bar{\alpha}(q^2)$ is a non-perturbative generalization of the canonical perturbative coupling $\alpha_s(q^2)$

⇒ it is intimately related to the phenomenon of dynamical gluon mass generation

■ The charge $\bar{\alpha}(q^2)$ provides the bridge leading from the deep ultraviolet regime to the deep infrared one

⇒ the definition of $\bar{\alpha}(q^2)$ is not unique: may be obtained in two ways

⇒ despite the distinct theoretical origins of $\bar{\alpha}(q^2)$, they coincide exactly in the deep infrared.

⇒ the ultimate reason for this is the existence of a non-perturbative identity relating various of the Green functions appearing in their respective definitions

■ For example, $\bar{\alpha}(q^2)$ can be obtained from the Schwinger-Dyson solutions for the gluon self-energy $\hat{\Delta}(q^2)$

⇒ in this definition the solutions for $\hat{\Delta}(q^2)$ are used to form a renormalization-group invariant quantity: $\hat{d}(q^2) = g^2 \hat{\Delta}(q^2)$

⇒ the inverse of $\hat{d}(q^2)$ quantity may be written

$$\hat{d}^{-1}(q^2) = \frac{[q^2 + m^2(q^2)]}{\bar{\alpha}(q^2)}$$

where now

$$\frac{1}{\bar{\alpha}(q^2)} = b_0 \ln \left(\frac{q^2 + m^2(q^2)}{\Lambda^2} \right)$$

■ Note that here b_0 is precisely the first coefficient of the QCD β function and Λ is the QCD mass scale

⇒ thus $\bar{\alpha}(q^2)$ has exactly the same form of the leading order (LO) perturbative QCD coupling:

$$\frac{1}{\alpha_s^{LO}(p^2)} = b_0 \ln \left(\frac{p^2}{\Lambda^2} \right)$$

if $q^2 + m^2(q^2) \rightarrow p^2$ in the argument of the logarithm

⇒ this will effectively ensure that, in practice, the QCD effective charge can be successfully obtained by saturating the perturbative strong coupling $\alpha_s^{LO}(q^2)$

■ That is to say,

$$\begin{aligned}\bar{\alpha}^{LO}(q^2) &= \alpha_s^{LO}(q^2) \Big|_{q^2 \rightarrow q^2 + m^2(q^2)} \\ &= \frac{1}{b_0 \ln \left(\frac{q^2 + m^2(q^2)}{\Lambda^2} \right)},\end{aligned}$$

where $b_0 = \beta_0/4\pi = (11C_A - 2n_f)/12\pi$

■ A next-to-leading order (NLO) effective charge can be built through the same procedure

$$\bar{\alpha}^{NLO}(q^2) = \frac{1}{b_0 \ln\left(\frac{q^2 + 4m^2(q^2)}{\Lambda^2}\right)} \left[1 - \frac{b_1}{b_0^2} \frac{\ln\left(\ln\left(\frac{q^2 + 4m^2(q^2)}{\Lambda^2}\right)\right)}{\ln\left(\frac{q^2 + 4m^2(q^2)}{\Lambda^2}\right)} \right],$$

where $b_1 = \beta_1/16\pi^2 = [34C_A^2 - n_f(10C_A + 6C_F)]/48\pi^2$

■ We investigate three different types of QCD effective charge

$$\bar{\alpha}^{NLO}(q^2)$$

⇒ they can be constructed from two independent dynamical gluon masses having distinct asymptotic behaviors:

$$m_{log}^2(q^2) = m_g^2 \left[\frac{\ln \left(\frac{q^2 + \rho m_g^2}{\Lambda^2} \right)}{\ln \left(\frac{\rho m_g^2}{\Lambda^2} \right)} \right]^{-1-\gamma_1}$$

and

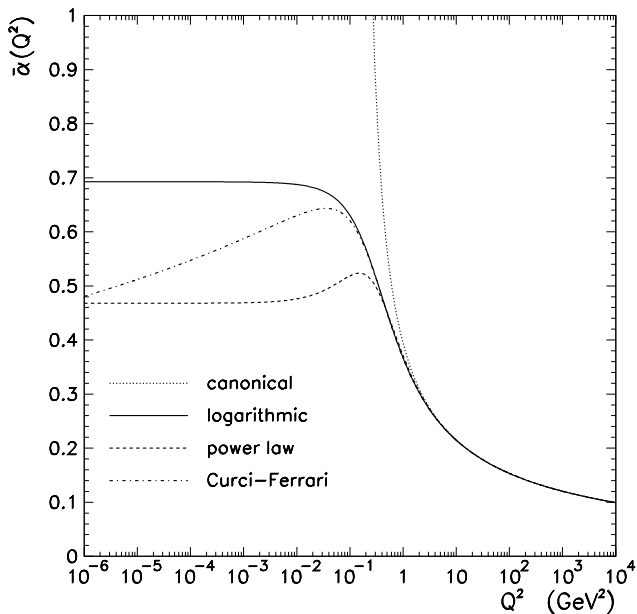
$$m_{pl}^2(q^2) = \frac{m_g^4}{q^2 + m_g^2} \left[\frac{\ln \left(\frac{q^2 + \rho m_g^2}{\Lambda^2} \right)}{\ln \left(\frac{\rho m_g^2}{\Lambda^2} \right)} \right]^{\gamma_2-1}$$

■ The first two QCD effective charges can be constructed simply by combining the above equations

■ The third effective charge vanishes logarithmically in the infrared, in agreement with some recent lattice results using a renormalization group invariant coupling resulting from a particular combination of the gluon and ghost propagators

$$\bar{\alpha}_{CF}(q^2) = \frac{1}{1 + c_0 \ln \left(1 + \frac{4m_{log}^2(q^2)}{q^2} \right)} \bar{\alpha}_{log}(q^2)$$

- It may be worth emphasizing that the QCD effective charges $\bar{\alpha}_{log}(q^2)$, $\bar{\alpha}_{pl}(q^2)$ and $\bar{\alpha}_{CF}(q^2)$ exhibit infrared fixed points as $q^2 \rightarrow 0$, i.e. the dynamical gluon mass tames the Landau pole
- In the limit $q^2 \gg \Lambda^2$ these effective charges match with the canonical perturbative two-loop coupling: $\bar{\alpha}(q^2 \gg \Lambda^2) \rightarrow \alpha_s(q^2)$
- The analyticity of $\bar{\alpha}_{log}(q^2)$, $\bar{\alpha}_{pl}(q^2)$ and $\bar{\alpha}_{CF}(q^2)$ is automatically preserved if the gluon mass scale is set larger than half of the QCD scale parameter, namely $m_g/\Lambda > 1/2$
- In a mathematical sense, the QCD effective charges belong to the class of holomorphic couplings



Canonical coupling and QCD effective charges at NLO

Results

■ The nucleon structure function $F_2(x, Q^2)$ has been measured in DIS of leptons off nucleons at the HERA collider

⇒ we carry out global fits to small- x $F_2(x, Q^2)$ data at low and moderate Q^2 values

⇒ we use HERA data from the ZEUS and H1 Collaborations, with the statistic and systematic errors added in quadrature

⇒ specifically, we fit to the structure function at $Q^2 = 0.2, 0.25, 0.3, 0.5, 0.65, 0.85, 1.2, 1.3, 1.5, 1.9, 2.0, 2.5, 3.5, 5.0, 6.5$ and 10 GeV^2

■ The global fits were performed using a χ^2 fitting procedure, adopting an interval $\chi^2 - \chi_{min}^2$ corresponding to the projection of the χ^2 hypersurface enclosing 90% of probability

■ We introduce a systematic expansion of the DIS cross sections in terms of $\alpha_s(Q^2)$, evaluated at the virtuality scale

⇒ this means that all the couplings $\alpha_s(Q^2)$ appearing in the calculations are replaced by QCD effective charges

⇒ in all the fits we fix $n_f = 3$ and $\Lambda = 284 \text{ MeV}$

⇒ the choice is $n_f = 3$ justified by the fact that most of the data lie at Q values below the charm mass m_c

⇒ in the $n_f = 3$ scheme the charm can only be pair-produced by gluon splittings when kinematically allowed

⇒ at the low scales of the data considered in the fits, production of charm is not kinematically allowed and therefore in the $n_f = 3$ scheme the charm quark decouples

Table: The values of the fitting parameters from the global fit to F_2 data. Results obtained using the **logarithmic effective charge**.

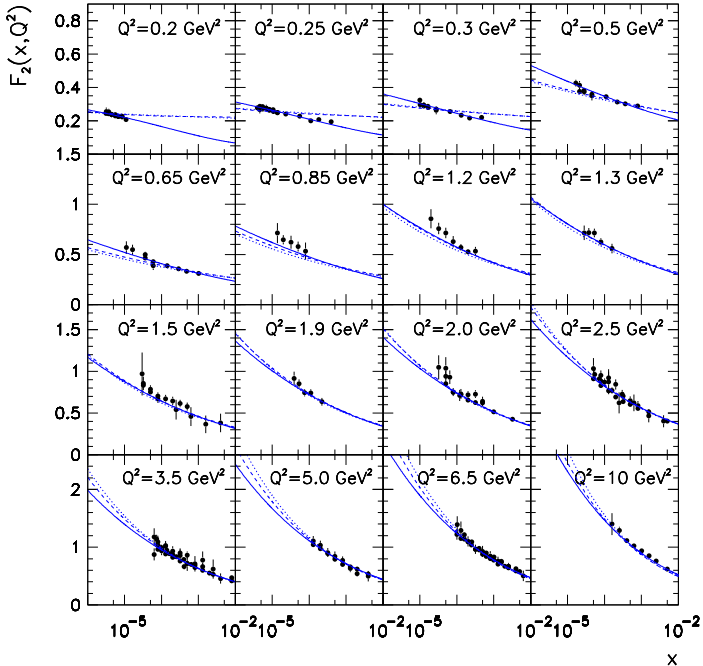
	τ_2	$\tau_2 + \tau_4$	$\tau_2 + \tau_4 + \tau_6$
m_g [MeV]	340 ± 17	284 ± 17	310 ± 53
Q_0^2 [GeV ²]	0.080 ± 0.048	0.54 ± 0.17	0.99 ± 0.16
A_g	0.091 ± 0.070	0.42 ± 0.24	1.19 ± 0.26
A_q	0.727 ± 0.054	0.60 ± 0.12	0.422 ± 0.086
$A_g^{\tau_4}$	-	0.59 ± 0.26	0.58 ± 0.19
$A_q^{\tau_4}$	-	0.020 ± 0.018	0.232 ± 0.081
$A_g^{\tau_6}$	-	-	0.139 ± 0.076
$A_q^{\tau_6}$	-	-	0.0203 ± 0.0082
ν	246	244	242
$\tilde{\chi}$	2.41	2.08	1.21

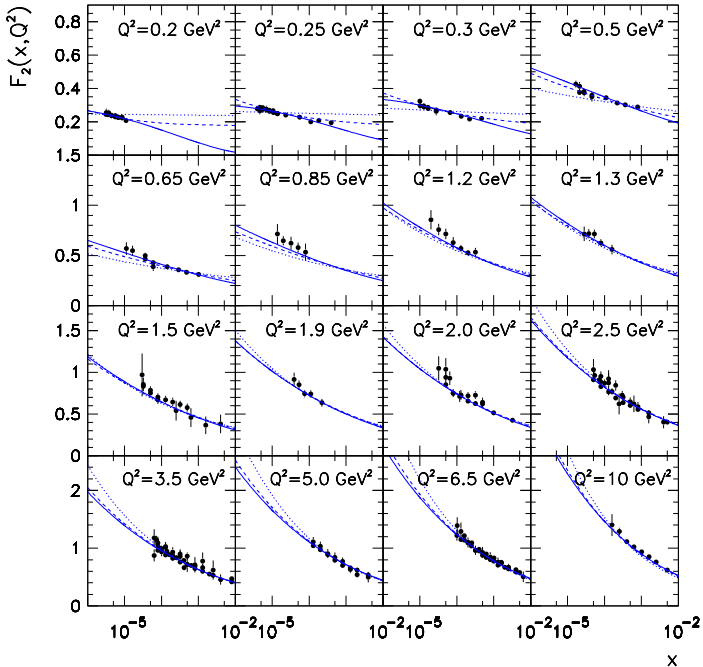
Table: The values of the fitting parameters from the global fit to F_2 data. Results obtained using the **power-law effective charge**.

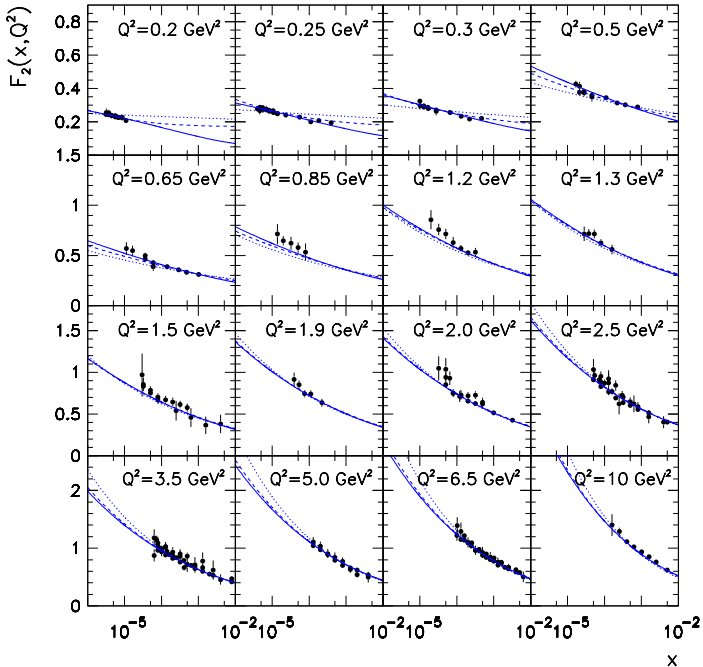
	τ_2	$\tau_2 + \tau_4$	$\tau_2 + \tau_4 + \tau_6$
m_g [MeV]	360 ± 9	282 ± 24	415 ± 67
Q_0^2 [GeV ²]	0.11 ± 0.15	0.929 ± 0.073	1.17 ± 0.19
A_g	-0.090 ± 0.031	0.856 ± 0.080	1.37 ± 0.34
A_q	0.857 ± 0.017	0.488 ± 0.042	0.403 ± 0.081
$A_g^{\tau_4}$	-	0.69 ± 0.14	0.39 ± 0.30
$A_q^{\tau_4}$	-	0.132 ± 0.013	0.38 ± 0.16
$A_g^{\tau_6}$	-	-	0.135 ± 0.073
$A_q^{\tau_6}$	-	-	0.040 ± 0.014
ν	246	244	242
$\tilde{\chi}$	2.88	1.38	1.19

Table: The values of the fitting parameters from the global fit to F_2 data. Results obtained using the **Curci-Ferrari effective charge**.

	τ_2	$\tau_2 + \tau_4$	$\tau_2 + \tau_4 + \tau_6$
m_g [MeV]	326 ± 72	234 ± 14	302 ± 53
Q_0^2 [GeV ²]	0.05 ± 1.35	0.883 ± 0.071	0.97 ± 0.16
A_g	0.09 ± 0.30	0.846 ± 0.075	1.19 ± 0.28
A_q	0.73 ± 0.31	0.491 ± 0.041	0.420 ± 0.091
$A_g^{\tau_4}$	-	0.65 ± 0.13	0.55 ± 0.19
$A_q^{\tau_4}$	-	0.1179 ± 0.0090	0.224 ± 0.082
$A_g^{\tau_6}$	-	-	0.131 ± 0.076
$A_q^{\tau_6}$	-	-	0.0194 ± 0.0078
ν	246	244	242
$\tilde{\chi}$	2.39	1.34	1.20



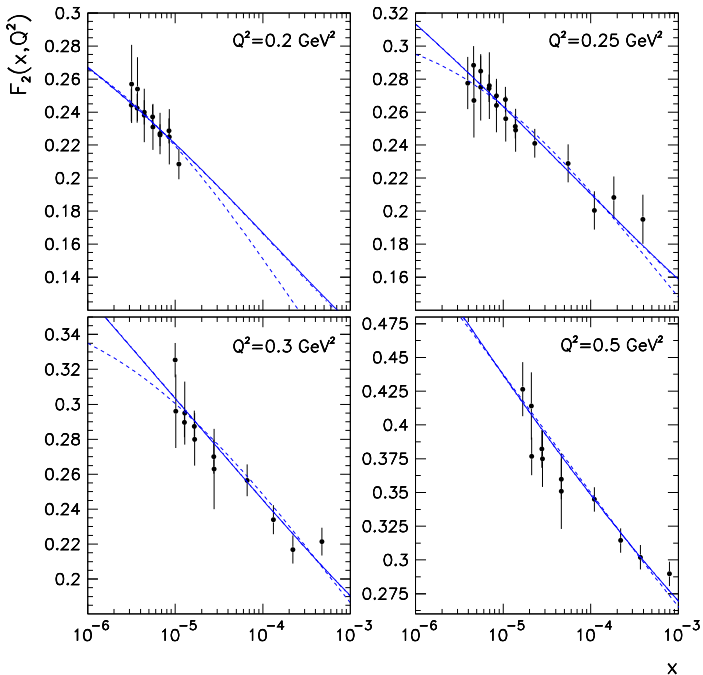


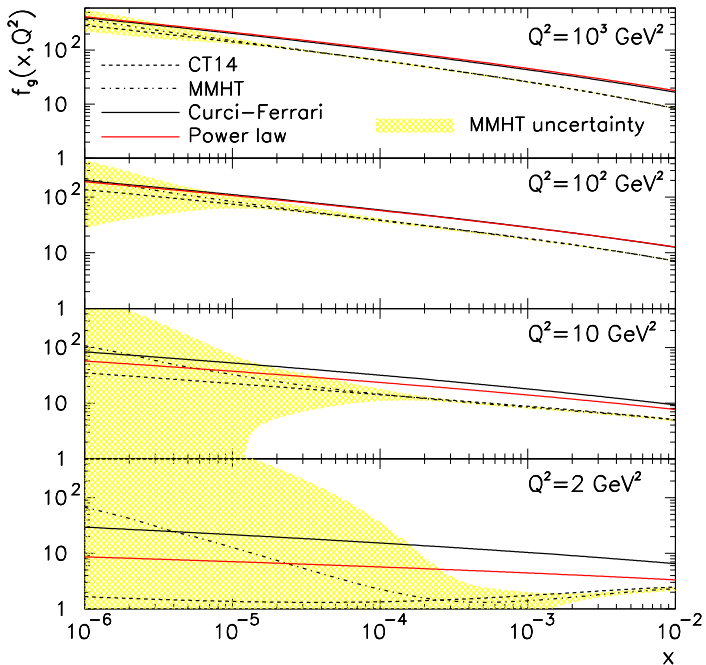


()

VII ONTQC

39 / 45





Conclusions and Perspectives

- We have obtained an analytical approach to calculating higher twist corrections to the structure function $F_2(x, Q^2)$

⇒ the formalism is based on existing analytical solutions of the DGLAP equation in the small x region

- Our analytical approach, when combined with some non-perturbative information from QCD, results in an instrumental tool to study structure functions at very small x region in the infrared regime

- Comparing the renormalon and standard GDFs, we see that our distributions $f_g(x, Q^2)$ are in good agreement with the CT14 and MMHT ones at very small x

Conclusions and Perspectives

- For inclusive $e^\pm p$ DIS process the real experimentally measured data are the reduced cross sections $\tilde{\sigma}$,

$$\frac{d^2\sigma^{e^\pm p}}{dx dQ^2} = \frac{2\pi\alpha^2 Y_+}{xQ^4} \tilde{\sigma}(x, Q^2, y),$$

where $\tilde{\sigma}(x, Q^2, y) = F_2(x, Q^2) - \frac{y^2}{Y_+} F_L(x, Q^2)$, y is the inelasticity, α is the fine structure constant and $Y_+ = 1 + (1 - y)^2$

⇒ F_L is usually treated as a small correction in the F_2 extraction from the reduced cross section $\tilde{\sigma}$

⇒ in our analysis the bias introduced by neglecting F_L is kept to a minimum

Conclusions and Perspectives

⇒ however F_L is an important quantity due to its rather direct relation to $f_g(x, Q^2)$

⇒ thus, it is clearly important to develop a consistent QCD method to describe directly the reduced cross section $\tilde{\sigma}$

⇒ work in this direction, using the renormalon approach is in progress

THANK YOU